Ionics (2015) 21:2155–2160
DOI 10.1007/s11581-015-1399-x

ORIGINAL PAPER

Enhanced electrochemical performance of Cu_2O-modified $Li_4Ti_5O_{12}$ anode material for lithium-ion batteries

Junsheng Wang · Fei Zhao · Jie Cao · Yu Liu ·
Baofeng Wang

Received: 4 September 2014 / Revised: 24 December 2014 / Accepted: 18 February 2015 / Published online: 7 March 2015

Abstract $Li_4Ti_5O_{12}/Cu_2O$ composite was prepared by ball milling $Li_4Ti_5O_{12}$ and Cu_2O with further heat treatment. The structure and electrochemical performance of the composite were investigated via X-ray diffraction, scanning electron microscopy, energy-dispersive spectroscopy, cyclic voltammetry, electrochemical impedance spectroscopy, and galvanostatic charge–discharge tests. $Li_4Ti_5O_{12}/Cu_2O$ composite exhibited much better rate capability and capacity performance than pristine $Li_4Ti_5O_{12}$. The discharge capacity of the composite at 2 C rate reached up to 122.4 mAh g^{-1} after 300 cycles with capacity retention of 91.3 %, which was significantly higher than that of the pristine $Li_4Ti_5O_{12}$ (89.6 mAh g^{-1}). The improvement can be ascribed to the Cu_2O modification. In addition, Cu_2O modification plays an important role in reducing the total resistance of the cell, which has been demonstrated by the electrochemical impedance spectroscopy analysis.

Keywords Cu_2O modification · $Li_4Ti_5O_{12}$ · Lithium-ion battery · Electrochemical performance

Introduction

Recently, Li-ion batteries (LIBs) have drawn significant attentions as the dominating candidates for electric vehicles (EVs) and hybrid electric vehicles (HEVs) with the potential to save oil and to decrease exhaust emissions [1, 2]. Currently, graphitic carbon is commonly used as anode materials in commercial LIBs. However, it suffers from a rather high irreversible capacity during the initial cycles and serious safety problems during repeated charge–discharge cycling [3, 4]. Spinel $Li_4Ti_5O_{12}$ (LTO) has been considered as an alternative anode material for LIBs because it can entirely eliminate potential safety issues due to its high and flat Li insertion voltage at ~ 1.55 V versus Li/Li^+, which prevents the growth of lithium dendrites and the decomposition of electrolyte as well as providing long cycle life and high reversibility [5, 6]. However, stable titanium oxides, including LTO, exhibit an inherently insulating property resulting from the presence of sole Ti^{4+}, which has a d^0 electronic configuration, seriously hindering its high rate performance [7]. Fortunately, satisfactory electrochemical performance of these materials can be achieved by either preparing nanosized LTO materials to reduce the physical diffusion length of electrons and Li ions [8–11] or surface modification and ion doping to enhance the Li-ion diffusion and electronic conductivity [12–16].

Carbon-free coatings, classified from surface modification, which enables superior rate performance, high tap density, and surface stability, has been recognized as one of the most effective techniques. It has been reported that the initial discharge capacity and cycling stability of $Li_4Ti_5O_{12}$ were improved by TiO_2 modification, suggesting that the existence of TiO_2 could improve the rate capability of $Li_4Ti_5O_{12}$ [17, 18]. The $Li_4Ti_5O_{12}$ electrodes with ZrO_2 coating exhibited higher specific capacity, better cycling performance, and rate capability than the pristine $Li_4Ti_5O_{12}$ [19]. However, to the best of our knowledge, there have been few reports on the performance improvement of the $Li_4Ti_5O_{12}$ by Cu_2O modification.

In this paper, using a facile solid-state method, a spinel $Li_4Ti_5O_{12}/Cu_2O$ composite was prepared and the effects of Cu_2O modification on the structure, morphology, and

---

J. Wang · F. Zhao · J. Cao · Y. Liu · B. Wang (✉)
Shanghai Key Laboratory of Materials Protection and Advanced Materials in Electric Power, Shanghai University of Electric Power, Shanghai 200090, China
e-mail: wangbaofeng@shiep.edu.cn

Y. Liu
CAS Key Laboratory of Materials for Energy Conversion, Shanghai Institute of Ceramics, CAS, Shanghai 200050, China

electrochemical performance of the $Li_4Ti_5O_{12}$ anode were intensively investigated.

Experimental

Preparation of pristine LTO and $Li_4Ti_5O_{12}/Cu_2O$ composites

All of the reactants were analytical grade without further purification. Pristine LTO was prepared by solid-state reaction. TiO_2 anatase and $LiOH \cdot H_2O$ (n_{Li}/n_{Ti}=4.1:5 by mole) were first mixed using a planetary high-energy ball milling machine (QM-2SP2 (2 L); Zhengxian, China) for 2 h at the speed of 450 rpm in ethanol. The mass ratio of the ball and initial material was 5:1, and the volume of ethanol was two times of initial materials. The obtained binary precursor slurry was dried at 110 °C. Then, the dried powder was calcinated at 800 °C with the heating rate of 3 °C min^{-1} and kept for 12 h under air atmosphere.

To synthesize the $Li_4Ti_5O_{12}/Cu_2O$ composite, Cu_2O (AR) and the prepared LTO powder were used as the raw materials. Cu_2O and LTO were mixed in ethanol for 2 h by planetary ball milling machine (QM-2SP2 (2 L)) to obtain a homogenously dispersed suspension and then air-dried at 110 °C. After that, the obtained mixture was calcinated in N_2 atmosphere at 400 °C for 3 h and slowly cooled down. Besides, the pristine LTO was also ball milled for comparison.

Material characterization

The crystal structure was characterized by X-ray diffraction (XRD) measurement (Rigaku D/Max-RB using Cu Kα radiation) at a scan rate of 4° min^{-1} with 2θ ranging from 10° to 80° at room temperature. Scanning electron microscope (SEM, SU-70; Japan) equipped with an energy-dispersive spectroscope (EDS) was used to observe the morphology of the composite and to analyze the composition and element distribution of anode materials. The microstructures were investigated using transmission electron microscopy (TEM) and high-resolution TEM (HRTEM) on a JEOL 2100 F instrument.

Electrochemical test

Electrochemical performances were performed using CR2016 coin-type half-cell assembled in an argon-filled glove box using a lithium metal as counter electrodes. The composite electrodes were prepared by mixing the active materials, acetylene black, and polyvinylidene fluoride (PVDF) binder in *N*-methyl-2-pyrrolidine (NMP) solvent at a weight ratio of 80:10:10. The slurry was evenly spread onto copper foil and dried at 100 °C in vacuum. Disks of 1.54 cm^2 were punched out of the foil, and the loading samples on each disk were kept at a similar level, which was about 5.0 mg. The electrolyte solution 1.0 M $LiPF_6$ was mixed with ethylene carbonate (EC), ethyl methyl carbonate (EMC), and dimethyl carbonate (DMC) at a volume ratio of 1:1:1. The charge–discharge characteristics of the cells were tested in the potential range of 1.0–2.5 V on a CT2001A cell test instrument (Land Electronic Co.) at room temperature. A CHI660C electrochemical workstation was used to measure the cyclic voltammetry (CV) curves and electrochemical impedance spectroscopy (EIS). The CV measurement was operated at 0.1 mV s^{-1} between 1.0 and 2.5 V, and the EIS analysis was performed at the amplitude of 5 mV and at the frequency from 100 kHz to 0.1 Hz.

Results and discussion

The XRD patterns of the pristine and Cu_2O-modified LTO powders are presented in Fig. 1. All the diffraction peaks of the LTO powders can be indexed as spinel lithium titanate (cubic phase, space group $Fd\overline{3}m$) in accordance with spinel $Li_4Ti_5O_{12}$ (JCPDS card no. 49-0207). Compared with LTO, their location and relative intensities appear to be unchanged after the Cu_2O modification, indicating that the crystal structure of the LTO powders is retained after Cu_2O modification. No peaks related to Cu_2O are obviously observed in the XRD patterns of modified LTO with 1, 2, and 3 wt% of Cu_2O, largely attributed to their low modification amounts. On the contrary, when the content of Cu_2O increased to 6 wt%, the Cu_2O diffraction peaks were detected, suggesting that Cu_2O was located on the surface of LTO rather than doped in the lattice of LTO. This is understandable since the Cu atoms are not expected to enter the lattice of LTO when the synthesis temperature is as low as 400 °C in our procedure.

Figure 2 presented the SEM images of the LTO powders before and after Cu_2O modification with varied amounts. It is clearly observed from Fig. 2a that the surface of the pristine

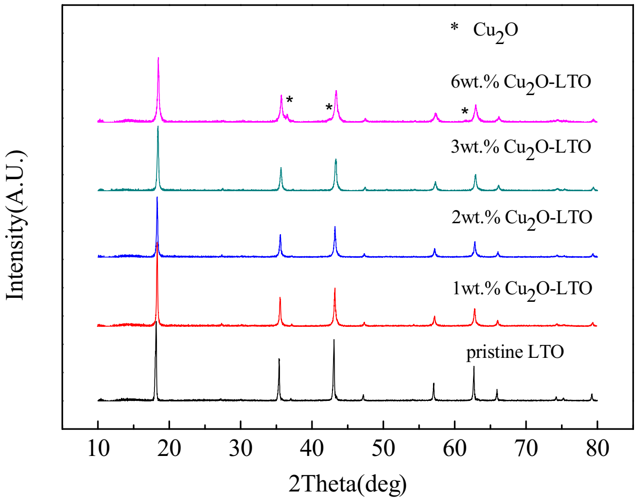

Fig. 1 XRD patterns of the pristine and Cu_2O-modified $Li_4Ti_5O_{12}$ powders

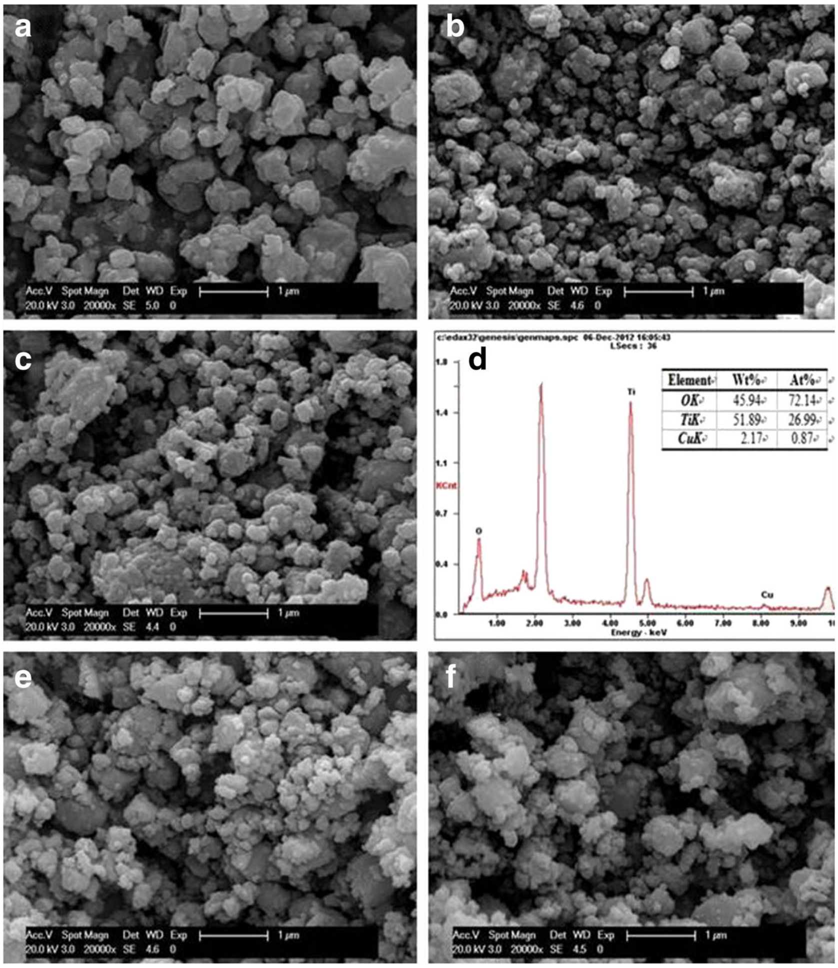

Element	Wt%	At%
OK	45.94	72.14
TiK	51.89	26.99
CuK	2.17	0.87

Fig. 2 SEM images of the **a** pristine; **b** 1 wt%, **c** 2 wt%, **e** 3 wt%, and **f** 6 wt% Cu_2O-modified $Li_4Ti_5O_{12}$ powders; and **d** EDS spectrum of 2 wt% Cu_2O-modified $Li_4Ti_5O_{12}$ powders

LTO particles is smooth and clean. In stark contrast, there are many small particles located on the periphery of LTO after being modified by Cu_2O with varied content (Fig. 2b, c, e, f) and the peak corresponding to Cu was detected through the EDS spectrum (Fig. 2d), verifying that the small particles are Cu_2O. As shown in Fig. 3, the dot elemental mappings

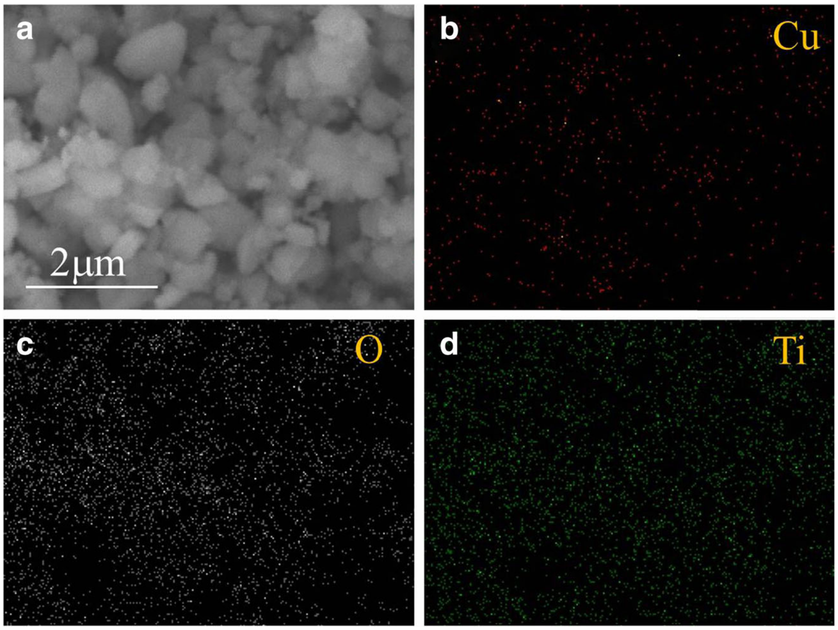

Fig. 3 The dot mapping of Cu, O, and Ti for LTO modified with 2 wt% Cu_2O

Fig. 4 TEM and HRTEM images of the 2 wt% Cu_2O–LTO material

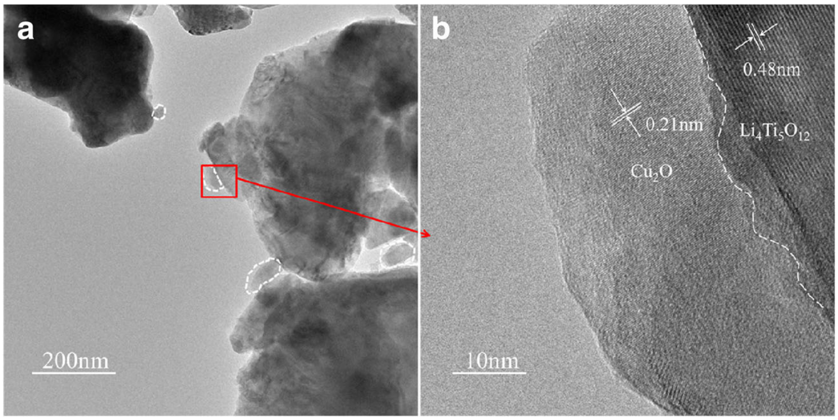

indicate the presence of Cu, Ti, and O elements in LTO modified with a 2 wt% Cu_2O sample. Obviously, Cu is dispersed uniformly in the sample as illuminated in Fig. 3b.

The detailed crystallographic structure of the samples was further analyzed by TEM and HRTEM. It is clear that the small particles are distributed around the bulks in Fig. 4a. The HRTEM images of the small particles are shown in Fig. 4b. Interlayer spacing of 0.21 nm was obtained, in good agreement with the lattice spacing of the (1 0 0) planes of Cu_2O. In addition, the d_{111} spacing of 0.48 nm is well matched with bulk spinel $Li_4Ti_5O_{12}$.

The cycling behavior and first charge–discharge curves of the samples between 1.0 and 2.5 V were displayed in Fig. 5a, b, respectively. It was apparent that the capacity performance and cycling stability of Cu_2O-modified LTO exceeded those of the pristine LTO. After 300 cycles, the

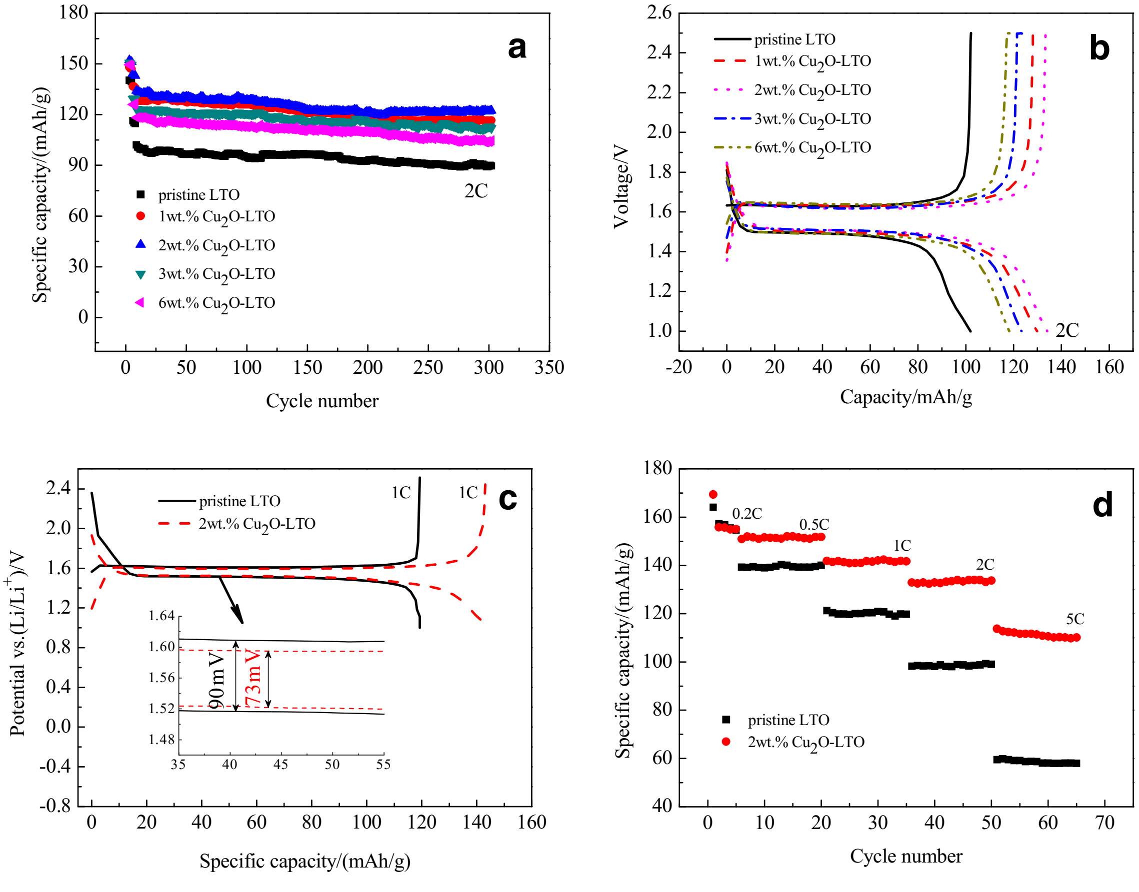

Fig. 5 **a** Cycle performance of the pristine $Li_4Ti_5O_{12}$ and Cu_2O-modified $Li_4Ti_5O_{12}$ electrodes at 2 C rate (the first 3 cycles were at 0.5 C rate, the 4th to 6th cycles were at 1 C rate). **b** The first charge–discharge profiles of the pristine $Li_4Ti_5O_{12}$ and Cu_2O-modified $Li_4Ti_5O_{12}$ electrodes at 2 C rate. **c** The first charge–discharge profiles of the pristine $Li_4Ti_5O_{12}$ and 2 wt% Cu_2O-modified $Li_4Ti_5O_{12}$ electrodes at 1 C rate (the *inset* shows the magnified region). **d** Comparison of the rate capabilities of $Li_4Ti_5O_{12}$ and 2 wt% Cu_2O-modified $Li_4Ti_5O_{12}$ electrode

capacity of the pristine LTO is only 89.6 mAh g^{-1}, while the capacity of LTO modified with 1, 2, 3, and 6 wt% Cu_2O were 116.5, 112.0, 122.4, and 104.7 mAh g^{-1}, respectively. The LTO modified with 2 wt% Cu_2O showed the best performance, which held 122.4 mAh g^{-1} after 300 cycles with capacity retention of 91.3 %. The high specific capacity is largely due to the contribution from Cu_2O in the composite which is considered as an anode material with high capacity [20]. The excellent stability of the composite material could be attributed to its enhanced electrical conductivity, which would be proven later by the EIS results.

The first charge–discharge profiles of the pristine LTO and 2 wt% Cu_2O-modified LTO at 1 C rate were shown in Fig. 5c. Both electrodes present voltage plateau around 1.55 V, which were the result of a two-phase reaction based on the redox couple of Ti^{3+}/Ti^{4+} during lithium-ion extraction and insertion process [21, 22]. It has been found that the polarization between the charge and discharge plateau was reduced from 90 mV for the sample of the pristine LTO to 73 mV for the sample of $Li_4Ti_5O_{12}/Cu_2O$, indicating that the kinetics of the pristine LTO were indeed improved after modification with 2 wt% Cu_2O. For the pristine LTO, the slow electrode reaction resulted in remarkable electrochemical polarization.

In addition, the rate capabilities of the pristine LTO and 2 wt% Cu_2O-modified LTO were also tested at different rates (Fig. 5d). As shown in Fig. 5d, the LTO/Cu_2O electrode delivered a capacity of 169.4, 150.9, 141.9, 132.9, and 113.7 mAh g^{-1} at 0.2, 0.5, 1, 2, and 5 C, respectively, while that of the LTO electrode was of 164.3, 139.9, 119.3, 98.7, and 59.5 mAh g^{-1} at the same rate. LTO/Cu_2O exhibited obviously improved capacity especially at a high rate. For LTO/Cu_2O, at the rate of 5 C, 67.1 % (113.7 mAh g^{-1}) of the discharge capacity at 0.2 C was reserved, while it was only 36.2 % (59.5 mAh g^{-1}) for pristine LTO. The significant improvement in the rate performance of LTO/Cu_2O arises from the Cu_2O modification that enhances the electrochemical activity of the composite.

To investigate the reason for the variation in their rate capabilities and capacity performances, the CVs for the pristine and 2 wt% Cu_2O-modified LTO sample were displayed in Fig. 6a. The peaks in Fig. 6a were derived from the structure transition from spinel to rock salt phase in the two samples. In other words, Cu_2O modification did not eliminate the phase transition. The potential difference between cathodic and anodic peak for 2 wt% Cu_2O-modified LTO (0.181 V) is smaller than that for LTO (0.237 V). Compared with the pristine one, the Cu_2O-modified anode had decreased peak difference and increased peak current. These results revealed that the Cu_2O modification not only reduced the polarization but also improved the electrochemical activity of the anode.

The role of the Cu_2O modification was further investigated by the EIS analysis. Figure 6b showed the typical Nyquist plots of the pristine and 2 wt% Cu_2O-modified LTO electrode after three charge–discharge cycles. Each plot included three parts. The first semicircle at the high-frequency region was relying on the resistance derived from Li^+ migration through solid–electrolyte interfacial (SEI) films (R_{sf}). It was found that the 2 wt% Cu_2O-modified anode had the relatively lower R_{sf} compared with that of the pristine one. The possible reason was that the interfacial structure of LTO had been changed after being modified with Cu_2O, which may further influence the properties of SEI layer, such as thickness and density [23]. The much more obvious difference between the two samples laid in the second semicircle in the medium-frequency region, which was assigned to the charge transfer resistance at the surface layer–anode particle interface (Rct). It has been reported that the cell impedance was dominated by Rct from the electrode material [24]. As shown in Fig. 6b, the semicircle diameters of LTO/C were much smaller than that of the pristine LTO, indicating that Cu_2O modification plays an important role in reducing the Rct of cell. The sloping line in the low-frequency range was attributed to the Warburg impedance, which was associated with Li^+ diffusion in the bulk electrode materials.

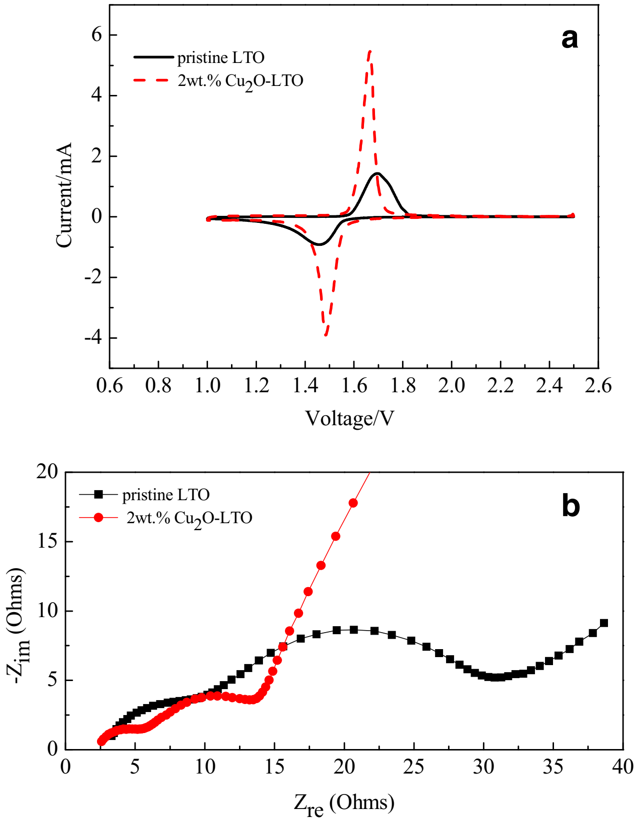

Fig. 6 **a** The CV curves of the anodes with a scan rate of 0.1 mV s^{-1}. **b** Impedance spectra of the anodes obtained after 3 cycles

Conclusions

Cu_2O-modified $Li_4Ti_5O_{12}$ composite was synthesized by using a facile solid-state method. The crystalline structure of the

Cu_2O-modified $Li_4Ti_5O_{12}$ anode shows no obvious change compared with the bare material; however, significantly improved electrochemical performance has been achieved. At 2 C rate, the 2 wt% Cu_2O-modified $Li_4Ti_5O_{12}$ composite delivered a discharge capacity of 122.4 mAh g^{-1} after 300 cycles. The CV results revealed that Cu_2O modification would not eliminate the phase transition but improve the electrochemical reversibility and activity of $Li_4Ti_5O_{12}$. Besides, EIS analysis showed that Cu_2O modification played an important role in reducing the impedance of the $Li_4Ti_5O_{12}/Cu_2O$ composite.

Acknowledgments This work has been carried out with the financial support of Shanghai Municipal Education Commission (“085” program) and Science and Technology Commission of Shanghai Municipality (No: 14DZ2261000).

References

1. Zhu GN, Chen L, Wang YG, Wang CX, Che RC, Xia YY (2013) Binary $Li_4Ti_5O_{12}$-$Li_2Ti_3O_7$ nanocomposite as an anode material for Li-ion batteries. Adv Funct Mater 23:640–647
2. Tarascon JM, Armand M (2001) Review article issues and challenges facing rechargeable lithium batteries. Nature 414:359–367
3. Shen LF, Li HS, Uchaker E, Zhang XG, Cao GZ (2012) General strategy for designing core–shell nanostructured materials for high-power lithium ion batteries. Nano Lett 12:5673–5678
4. Zhu YR, Yin LC, Yi TF, Liu HP, Xie Y, Zhu RS (2013) Electrochemical performance and lithium-ion intercalation kinetics of submicron-sized $Li_4Ti_5O_{12}$ anode material. J Alloys Compd 547:107–112
5. Cheng L, Liu HJ, Zhang JJ, Xiong HM, Xia YY (2006) Nanosized $Li_4Ti_5O_{12}$ prepared by molten salt method as an electrode material for hybrid electrochemical supercapacitors. J Electrochem Soc 153:A1472–A1477
6. Shen LF, Uchaker E, Zhang XG, Cao GZ (2012) Hydrogenated $Li_4Ti_5O_{12}$ nanowire arrays for high rate lithium ion batteries. Adv Mater 24:6502–6506
7. Ouyang CY, Zhong ZY, Lei MS (2007) Ab initio studies of structural and electronic properties of $Li_4Ti_5O_{12}$ spinel. Electrochem Commun 9:1107–1112
8. Yan H, Zhu Z, Zhang D, Li W (2012) A new hydrothermal synthesis of spherical $Li_4Ti_5O_{12}$ anode material for lithium-ion secondary batteries. J Power Sources 219:45–51
9. Liu GY, Wang HY, Liu GQ, Yang ZZ, Jin B, Jiang QC (2012) Facile synthesis of nanocrystalline $Li_4Ti_5O_{12}$ by microemulsion and its application as anode material for Li-ion batteries. J Power Sources 220:84–88
10. Tang YF, Yang L, Qiu Z, Huang JS (2008) Preparation and electrochemical lithium storage of flower-like spinel $Li_4Ti_5O_{12}$ consisting of nanosheets. Electrochem Commun 10:1513–1516
11. Wu FX, Li XH, Wang ZX, Guo HJ, He ZJ, Zhang Q, Xiong XH, Yue P (2012) Low-temperature synthesis of nano-micron $Li_4Ti_5O_{12}$ by an aqueous mixing technique and its excellent electrochemical performance. J Power Sources 202:374–379
12. Vujkovic M, Stojkovic I, Mitric M (2013) Hydrothermal synthesis of $Li_4Ti_5O_{12}$/C nanostructured composites: morphology and electrochemical performance. Mater Res Bull 48:218–223
13. Wang J, Zhao HL, Yang Q, Wang CM, Lv PP, Xia Q (2013) $Li_4Ti_5O_{12}$–TiO_2 composite anode material for lithium-ion batteries. J Power Sources 222:196–201
14. Tian BB, Xiang HF, Zhang L, Wang HH (2012) Effect of Nb-doping on electrochemical stability of $Li_4Ti_5O_{12}$ discharged to 0 V. J Solid State Electrochem 16:205–211
15. Wu HB, Chang S, Liu XL, Yu LQ, Wang GL, Cao DX, Zhang YM, Yang BF, She PL (2013) Sr-doped $Li_4Ti_5O_{12}$ as the anode material for lithium-ion batteries. Solid State Ionics 232:13–18
16. Yi TF, Shu J, Zhu YR, Zhu XD, Yue CB, Zhou AN, Zhu RS (2009) High-performance $Li_4Ti_{5-x}V_xO_{12}$ ($0\leq x\leq 0.3$) as an anode material for secondary lithium-ion battery. Electrochim Acta 54:7464–7470
17. Liu GY, Wang HY, Liu GQ, Yang ZZ, Jin B, Jiang QC (2013) Synthesis and electrochemical performance of high-rate dual-phase $Li_4Ti_5O_{12}$–TiO_2 nanocrystallines for Li-ion batteries. Electrochim Acta 87:218–223
18. Liao JY, Xiao XC, Higgins D, Lee DG, Hassan F, Chen ZW (2013) Hierarchical $Li_4Ti_5O_{12}$-TiO_2 composite microsphere consisting of nanocrystals for high power Li-ion batteries. Electrochim Acta 108:104–111
19. Liu J, Li XF, Cai M, Li RY, Sun XL (2013) Ultrathin atomic layer deposited ZrO_2 coating to enhance the electrochemical performance of $Li_4Ti_5O_{12}$ as an anode material. Electrochim Acta 93:195–201
20. Zhou XY, Shi JJ, Liu Y, Su QM, Zhang J, Du GH (2014) Microwave-assisted synthesis of hollow CuO–Cu_2O nanosphere/graphene composite as anode for lithium-ion battery. J Alloys Compd 615:390–394
21. Ma S, Noguchi H (2001) Electrochemical properties of $LiFe_5O_8Li_4Ti_5O_{12}$ solid solution. J Electrochem Soc 148:A589–A594
22. Bach S, Pereira-Ramos JP, Baffier N (1999) Electrochemical properties of sol–gel $Li_{4/3}Ti_{5/3}O_4$. J Power Sources 81–82:273–276
23. Chen JM, Cho YD, Hsiao CL, Fey GTK (2009) Electrochemical studies on $LiCoO_2$ surface coated with $Y_3Al_5O_{12}$ for lithium-ion cells. J Power Sources 189:279–287
24. Chen CH, Liu J, Amine K (2001) Symmetric cell approach and impedance spectroscopy of high power lithium-ion batteries. J Power Sources 96:321–328